A novel generalized dispersion equation to design circumferential wave fluid sensors

J. Y. Le Pommellec[1] · **A. El Baroudi**[1]

Abstract
A novel analytical investigation of circumferential (i.e. torsional) wave propagation in long anisotropic cylindrical rod (waveguide), surrounded by a viscoelastic fluid is proposed. The material is transversely isotropic, with its symmetry axis coincident with the axial axis of the cylindrical rod. In particular, a new form of the complex dispersion equation is presented. The aim of this paper is to study the correlation between the rheological properties of the fluid and the wave characteristics (phase and attenuation). The effect of the frequency and the waveguide radius on the wave characteristics are highlighted. The obtained results show that the measurements should be performed at high frequency using small rod radius. Accordingly, the results can be serve as benchmark solutions in design of torsional wave fluid sensors.

Keywords Circumferential wave · Transversely isotropic material · Viscoelastic fluid

1 Introduction

The concept of circumferential wave dipstick is attractive in industry for fluid characterizations. The idea is that the wave propagation in a solid elastic rod can sense the fluid rheological properties. The circumferential wave which propagates along the waveguide interacts with fluid boundary, it follows that the circumferential wave properties (velocity and attenuation) are highly affected [1].

The circumferential elastic waves in dry cylinders has been studied by many authors [2–4]. They have investigated the material properties effects on the phase velocity of the circumferential modes. Huiling et al. have developed a theoretical model of guided circumferential waves propagating in double-walled carbon nanotubes [5]. They studied the dispersion curves of the guided circumferential wave propagation. Xu et al. have modeled the torsional wave propagation along a micro-tube with elastic membrane attached to its inner surface. They have presented numerically the dispersion diagram of the lowest-order wave with the membrane surface effect [6]. The interaction between the circumferential waves and viscous fluid has been considered by [7–11]. Nevertheless, the interaction modeling between the circumferential wave and a viscoelastic fluid is still lacking. Indeed, in the field of chemistry [12], medical diagnostics [13], or industrial monitoring [14], it is necessary to characterize the fluid viscoelasticity. One interesting application is the monitoring of polymerization [15]. During the process, the material changes from viscous fluid to elastic solids. This modification affects the propagation of the circumferential waves in a immersed circular rod.

Circumferential waves in elastic waveguide have been widely exploited to measure the fluid viscosity [1, 11, 16, 17]. However, in these papers the character viscoelastic of fluid has not been taken into account. A novel approach based on the exact theory, to be able to accurately predict the circumferential wave behavior in elastic waveguide loaded on its surface with a viscoelastic fluid, remains a daunting task and is the purpose of the present paper. The effects of frequency and waveguide radius on the phase velocity and attenuation of circumferential waves are investigated. The obtained curves show that the attenuation is much more sensitive than phase velocity to

✉ A. El Baroudi, adil.elbaroudi@ensam.eu | [1]Arts et Métiers ParisTech, 2 Boulevard du Ronceray, 49035 Angers, France.

https://doi.org/10.1007/s42452-019-0824-6

glycerol concentration. Otherwise, the sensitivity is more significant for small waveguide radius and high frequencies. These results can provide interesting information to design sensors: we can use circumferential wave propagation at high frequency (100 kHz) in anisotropic waveguide with small radius (1 mm).

2 Physical model description

To describe the waveguide structure that guides circumferential waves, we consider a two-layer system consisting of a viscoelastic fluid and an anisotropic cylindrical rod as shown in Fig. 1. The length of the waveguide is much greater than the radius a of the cross-section so that the interaction of the right-end face with the viscoelastic fluid is negligible [11]. Therefore, the current work focuses on the circumferential modes. The circumferential waves exhibit a multimode character, the fundamental mode plays an important role in many application such as NDT and sensors. Accordingly, in this work, the attention is focused on the properties of the fundamental mode of circumferential waves. For this set of modes, the non-zero components of displacement and velocity are u_θ and v_θ. Moreover, due to the axisymmetry of the studied modes, the velocity field, $\mathbf{v}(r,\theta,z) = \left(0, v_\theta, 0\right)$, and displacement field, $\mathbf{u}(r,\theta,z) = \left(0, u_\theta, 0\right)$, are independent of the θ variable and can be displayed in the (r, z) plane. Note that in previous works the circumferential vibration in an isotropic elastic cylinder was used to determine fluid viscosity. In the present work a novel theoretical approach is developed taking into account both the fluid viscoelasticity and anisotropy of the waveguide.

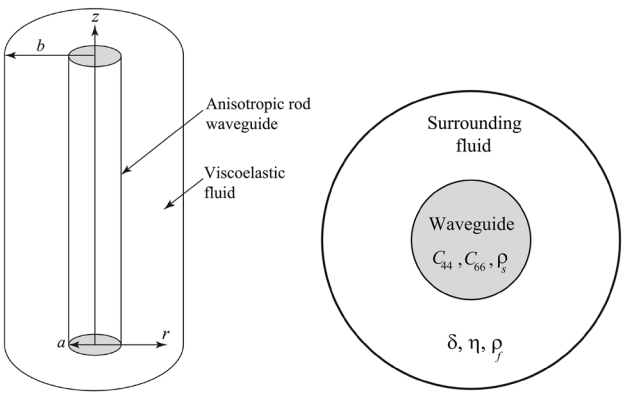

Fig. 1 The model geometry of anisotropic cylindrical rod waveguide. ρ_s, C_{44} and C_{66} correspond to the density and elastic constants of the cylindrical rod. The surface of the anisotropic cylinder is loaded by a viscoelastic fluid. The boundary between the anisotropic cylinder and viscoelastic fluid is at $r = a$. For viscoelastic fluid, δ, η and ρ_f are, respectively, relaxation time, dynamic viscosity and density

2.1 Mathematical formulation of waveguide

Based on the elastodynamic theory, the equation describing the motion of torsional vibrations of the waveguide in the absence of body forces is governed by

$$\frac{\partial \sigma_{r\theta}}{\partial r} + \frac{2\sigma_{r\theta}}{r} + \frac{\partial \sigma_{z\theta}}{\partial z} = \rho_s \frac{\partial^2 u_\theta}{\partial t^2} \tag{1}$$

where ρ_s is density, u_θ is displacement components along circumferential directions, and $\sigma_{\theta z}$, $\sigma_{r\theta}$, are the stress components and can be written using generalized Hooke's law as

$$\sigma_{\theta z} = C_{44}\frac{\partial u_\theta}{\partial z}, \quad \sigma_{r\theta} = C_{66}\left(\frac{\partial u_\theta}{\partial r} - \frac{u_\theta}{r}\right) \tag{2}$$

where C_{44} and C_{66} are the elastic coefficients. Substituting Eq. (2) in Eq. (1), yields the following partial differential equation

$$\frac{\partial^2 u_\theta}{\partial r^2} + \frac{1}{r}\frac{\partial u_\theta}{\partial r} - \frac{u_\theta}{r^2} + \frac{C_{44}}{C_{66}}\frac{\partial^2 u_\theta}{\partial z^2} = \frac{\rho_s}{C_{66}}\frac{\partial^2 u_\theta}{\partial t^2} \tag{3}$$

Note that in the case of an isotropic waveguide, $C_{44} = C_{66} = \mu$, the Lamé constant.

2.2 Mathematical formulation of viscoelastic fluid

In this study, we consider that the fluid velocity is small compared to the dimensions of the model, it then follows that all nonlinear convective inertia effects in the Navier–Stokes equation (NSE) can be neglected, therefore the linearized NSE takes the form

$$\rho_f \frac{\partial \mathbf{v}}{\partial t} = \nabla \cdot \boldsymbol{\tau} \tag{4}$$

where $\mathbf{v}$ is the velocity vector, t is the time, ρ_f is the density and $\boldsymbol{\tau}$ is the shear stress tensor. In this paper Maxwell model is adopted to describe the fluid viscoelasticity. Therefore, the differential equation for the relation between force and deformation can be written as [18]

$$\delta \frac{\partial \boldsymbol{\tau}}{\partial t} + \boldsymbol{\tau} = 2\eta \boldsymbol{\varepsilon}(\mathbf{v}) \tag{5}$$

where δ is the relaxation time, η is the dynamic viscosity and $\boldsymbol{\varepsilon}$ is the strain rate tensor. Applying the divergence operator to both sides of Eq. (5) and taking into account Eq. (4), we get the following viscoelastic fluid equation expressed in terms of the circumferential component of the velocity field

$$\frac{\partial^2 v_\theta}{\partial r^2} + \frac{1}{r}\frac{\partial v_\theta}{\partial r} - \frac{v_\theta}{r^2} + \frac{\partial^2 v_\theta}{\partial z^2} = \frac{\rho_f}{\eta}\left(\frac{\partial v_\theta}{\partial t} + \delta\frac{\partial^2 v_\theta}{\partial t^2}\right) \tag{6}$$

The Eq. (6) is known as the telegraph equation.

2.3 General solution of wave equations

For a circumferential harmonic wave propagation in the z-direction, the solution of Eqs. (3) and (6) (waveguide displacement u_θ and viscoelastic fluid velocity v_θ) are sought in the form

$$\left\{ \begin{array}{c} v_\theta \\ u_\theta \end{array} \right\}(r,z,t) = \left\{ \begin{array}{c} V(r) \\ U(r) \end{array} \right\} e^{j(kz-\omega t)} \tag{7}$$

where $k = k_0 + j\alpha$ is the complex wave number. Note that the real part of the wave number k_0 determines the circumferential wave phase velocity, and the imaginary part α represents the circumferential wave attenuation in the propagation direction. After substitution of Eq. (7) into Eqs. (3) and (6), the radial dependence can be expressed as

$$V(r) = BI_1(\beta_f r) + CK_1(\beta_f r), \quad U(r) = AI_1(\beta_s r)$$

where A, B and C are arbitrary amplitudes, I_1 and K_1 are modified Bessel functions of the first and second kind, and β_s and β_f are the radial wavenumbers

$$\beta_f = \sqrt{k^2 - \frac{2j}{d^2}(1-j\omega\delta)}, \quad \beta_s = \sqrt{\frac{C_{44}}{C_{66}}\left(k^2 - \frac{\omega^2}{c_s^2}\right)}$$

where $d = \sqrt{2\eta/(\rho_f\omega)}$ defines the fluid penetration depth [19], and $c_s = \sqrt{C_{44}/\rho_s}$ is the shear wave velocity in the waveguide. Thus, using Eqs. (2) and (5) the shear stress components that will be used in boundary conditions are given by

$$\begin{aligned} \left\{ \begin{array}{c} \tau \\ \sigma_{r\theta} \end{array} \right\}(r,z,t) &= \left\{ \begin{array}{c} \dfrac{\eta}{1-j\omega\delta}\left(\partial_r v_\theta - \dfrac{v_\theta}{r}\right) \\ C_{66}\left(\partial_r u_\theta - \dfrac{u_\theta}{r}\right) \end{array} \right\} \\ &= \left\{ \begin{array}{c} \dfrac{\eta}{1-j\omega\delta}\Sigma_f(r) \\ C_{66}\Sigma_s(r) \end{array} \right\} e^{j(kz-\omega t)} \end{aligned} \tag{8}$$

where the radial dependence is defind as

$$\Sigma_f(r) = \beta_f\left[BI_2(\beta_f r) + CK_2(\beta_f r)\right], \quad \Sigma_s(r) = \beta_s AI_2(\beta_s r)$$

2.4 Complex dispersion equation

In this paragraph boundary conditions must be used to determine the constants A, B and C. Assuming wall outer fluid surface, one can write : (i) continuity of velocity and shear stress at the interface between viscoelastic fluid and waveguide

$$\left(v_\theta + j\omega u_\theta\right)_{r=a} = 0 \tag{9}$$

$$\left(\tau - \sigma_{r\theta}\right)_{r=a} = 0 \tag{10}$$

(ii) wall outer surface of viscoelastic fluid is assumed

$$v_\theta\big|_{r=b} = 0 \tag{11}$$

By substituting Eqs. (7) and (8) into these boundary conditions provides three homogeneous and linear equations for the constants A, B and C. This system of equations has a nontrivial solution if the determinant of the coefficients equals zero. This leads to the following complex dispersion equation

$$\begin{aligned} &\frac{j\omega\eta\beta_f}{1-j\delta\omega} I_1(\beta_s a)\left[I_2(\beta_f a)K_1(\beta_f b) + I_1(\beta_f b)K_2(\beta_f a)\right] \\ &\quad + C_{66}\beta_s I_2(\beta_s a)\left[I_1(\beta_f a)K_1(\beta_f b) - I_1(\beta_f b)K_1(\beta_f a)\right] = 0 \end{aligned} \tag{12}$$

Equation (12) represents the complex dispersion equation of circumferential waves propagating in waveguide loaded with a viscoelastic fluid. For given dimensions, elastic waveguide constants and fluid properties, Eq. (12) constitutes an implicit transcendental function of k. The complex roots k may be computed using Mathematica software for a first mode vibration. After finding the real part k_0 and the imaginary part α of the wavenumber, the circumferential wave phase velocity $c_p = \omega/k_0$ can be calculated. As a remark, for a semi-infinite viscoelastic fluid, the complex dispersion equation (12) becomes

$$\frac{j\omega\eta\beta_f}{1-j\delta\omega} I_1(\beta_s a)K_2(\beta_f a) - C_{66}\beta_s I_2(\beta_s a)K_1(\beta_f a) = 0 \tag{13}$$

In the case of a viscous Newtonian fluid, the complex dispersion equation (13) takes the following form

$$j\omega\eta\beta_f I_1(\beta_s a)K_2(\beta_f a) - \mu\beta_s I_2(\beta_s a)K_1(\beta_f a) = 0 \tag{14}$$

which was previously obtained by Kim and Bau [11] for an isotropic waveguide.

3 Results and discussion

The same material properties used in [20, 21] and given in Table 1 for viscoelastic fluid were taken to construct this numerical example. The waveguide parameters were derived from [22] are given in Table 2. In this work, numerical calculations are performed in the frequency range from 1 to 50 (kHz) and for five values of glycerol concentrations 0, 71, 85, 95 and 100%. Table 3 highlighted the influence of glycerol concentration in water on the phase velocity and attenuation of the wave calculated using the dispersion equation (12). It can be seen from Table 3 that for each frequency, the phase velocity decreases with the glycerol concentration while the attenuation increases. As a

Table 1 Material parameters used for water–glycerol mixtures

χ (%)	η (Pa s)	ρ_f (kg/m^3)	δ (ps)
0	0.000894	1000	0.647
36	0.0027	1090	1.87
56	0.00527	1140	3.51
71	0.02	1190	12.7
80	0.0447	1210	27.1
85	0.0923	1220	54.2
95	0.452	1250	243
100	0.988	1260	500

χ is the concentration of glycerol in water

Table 2 Material parameters used for anisotropic cylindrical rod (waveguide)

	ρ_s (kg/m^3)	C_{44} (Pa)	C_{66} (Pa)	c_s (m/s)
Anisotropic rod	2800	2.850×10^{10}	2.345×10^{10}	3190.39

remark, for a zero glycerol concentration (pure water), the phase velocity is very close to the shear wave velocity in the waveguide c_s (see Table 2). When the glycerol concentration increases the phase velocity slowly decreases, and the attenuation significantly increases.

The effect of the frequency on the phase velocity and attenuation is depicted on Fig. 2. It is seen from Fig. 2 that the phase velocity increases with frequency and tends towards waveguide shear velocity c_s. It is also shown that the attenuation increases with the frequency. Otherwise, for a given frequency, the phase velocity decreases with the glycerol concentration while the attenuation augments. Finally, we can see that the attenuation is much more sensitive than phase velocity to glycerol concentration. The results highlighted in Fig. 2 can be justified by the influence of frequency on the penetration depth of the circumferential wave in the viscoelastic fluid. When the frequency augments the penetration decreases and the influence of the glycerol concentration on the phase velocity decreases. For high frequency this influence is negligible and the phase velocity is approximatively equal to the waveguide shear velocity c_s. Otherwise, the decreasing of the penetration depth linked to the frequency generates an increasing of the attenuation. Consequently, this attenuation is much more sensitive to glycerol concentration for high frequencies.

Waveguide radius is an another essential parameter in design of circumferential wave sensors. The influence of the rod radius on the phase velocity and attenuation is shown on Figs. 3 and 4. It can be seen from these figures

Table 3 Phase velocity c_p and attenuation α with $a = 3$ (mm)

χ (%)	$f = 1$ (kHz)		$f = 10$ (kHz)		$f = 50$ (kHz)	
	c_p (m/s)	α (Np/m)	c_p (m/s)	α (Np/m)	c_p (m/s)	α (Np/m)
0	3183.99	0.004	3188.36	0.013	3189.48	0.028
71	3157.66	0.021	3179.97	0.065	3185.72	0.145
85	3120.01	0.047	3167.81	0.143	3180.25	0.316
95	3036.50	0.111	3140.23	0.326	3167.77	0.715
100	2966.22	0.172	3116.47	0.492	3156.93	1.069

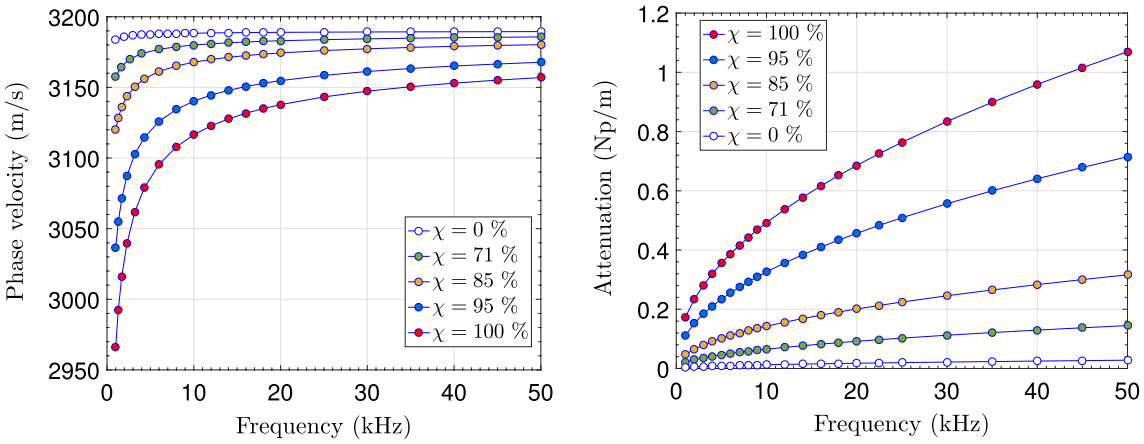

Fig. 2 Phase velocity and attenuation versus frequency for $a = 3$ (mm)

that the phase velocity increases with the rod radius and reach shear wave velocity in the waveguide c_s (Fig. 3). Otherwise, the attenuation decreases in a monotonous way (Fig. 4). For each radius value, phase velocity decreases with glycerol concentration while attenuation increases. This effect is more significant for low radius values.

The effect of the glycerol mass fraction on the phase velocity and attenuation is shown on Figs. 5 and 6. The calculations are performed for frequency range from 1 to 100 kHz and two rod radius 1 and 6 mm. Each curve shows two regions :

- For glycerol concentration less than about 40%, the phase velocity (Fig. 5) is approximatively equal to the shear wave velocity c_s in the waveguide (Table 2). Otherwise, the attenuation (Fig. 6) is negligible. The influence of the frequency value is very low.
- For the glycerol mass fraction exceeding 40%, the phase velocity decreases with mass fraction while the attenuation augments. These behaviors are more significant for small rod radius ($a = 1$ mm) and high frequency. We can see that the attenuation is much more sensitive than phase velocity to glycerol concentration.

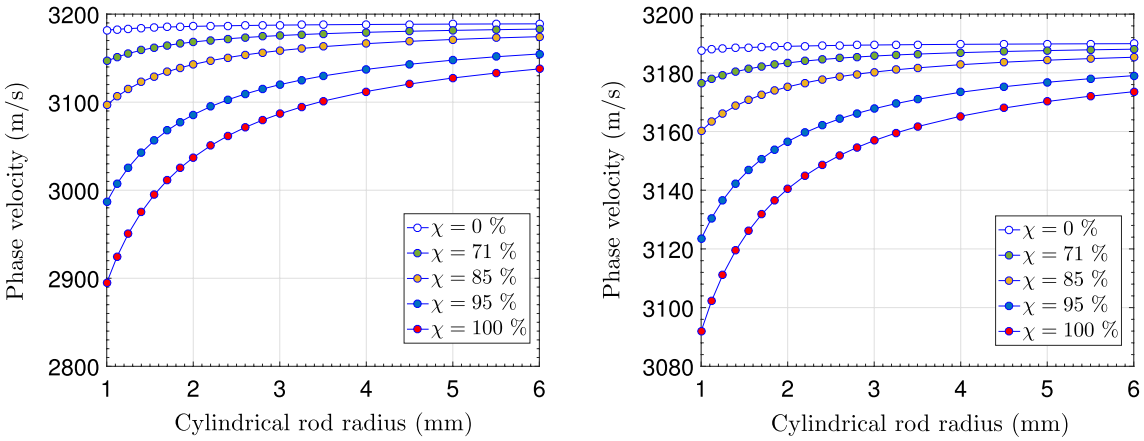

(a) $f = 5$ (kHz) **(b)** $f = 50$ (kHz)

Fig. 3 Phase velocity versus cylindrical rod radius

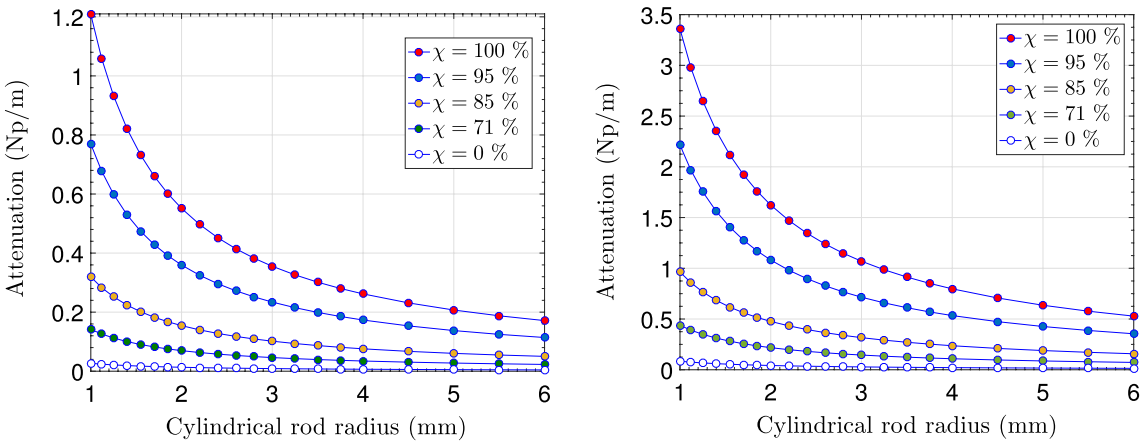

(a) $f = 5$ (kHz) **(b)** $f = 50$ (kHz)

Fig. 4 Attenuation versus cylindrical rod radius

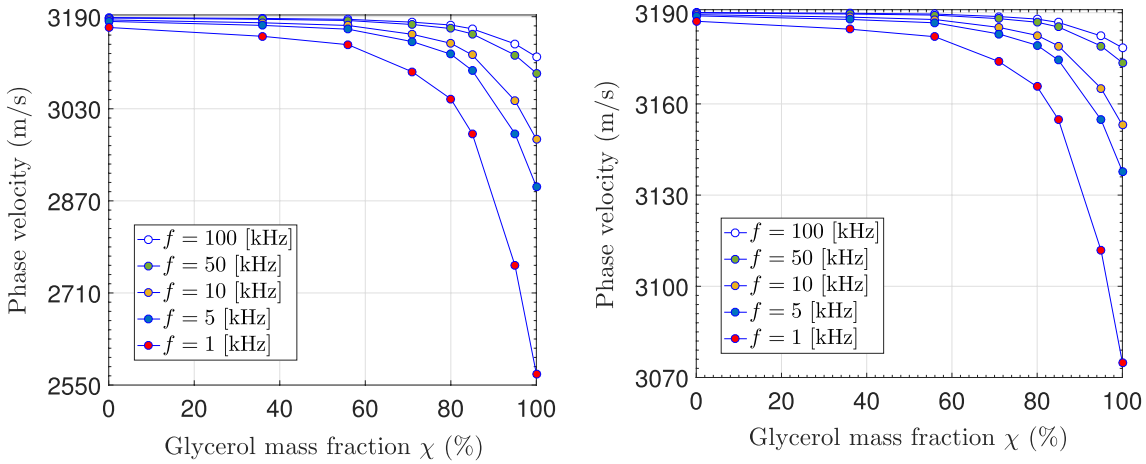

Fig. 5 Phase velocity versus glycerol mass fraction

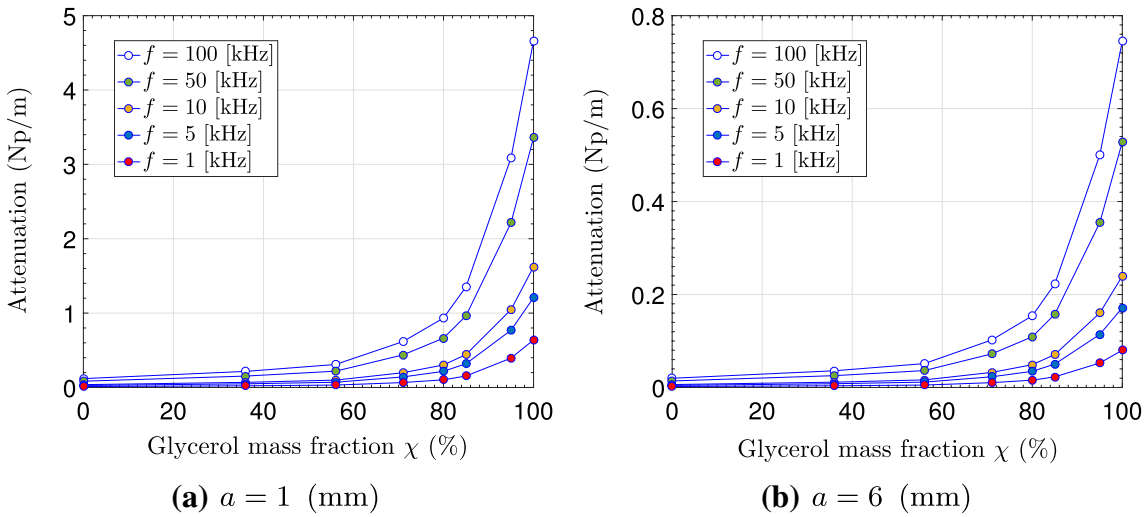

Fig. 6 Attenuation versus glycerol mass fraction

4 Conclusions

In this paper a novel analytical approach was used for the study of an anisotropic cylindrical rod (waveguide) surrounded by a viscoelastic fluid (water–glycerol mixture). A new complex dispersion equation was developed. Therefore, the graphs highlighted the influence of the frequency and waveguide radius on the phase velocity and attenuation for different values of glycerol concentrations. The glycerol concentration effect was also depicted for two waveguide radius (1 mm and 6 mm) and frequency ranging from 1 to 100 kHz. The obtained curves show that the attenuation is much more sensitive than phase velocity to glycerol concentration. Otherwise, The sensitivity is more significant for small waveguide radius and high frequency. Consequently, the characterization of a viscoelastic fluid can be performed using torsional wave propagation at high frequency in anisotropic waveguide with small radius.

Compliance with ethical standards

Conflict of interest The authors declare that they have no conflict of interest.

References

1. Kim JO, Wang Y, Bau HH (1991) The effect of an adjacent viscous fluid on the transmission of torsional stress waves in a submerged waveguide. J Acoust Soc Am 89(3):1414–1422
2. Kaul RK, Shaw RP (1981) Torsional waves in an axially homogeneous bimetallic cylinder. Int J Solids Struct 17:379–394
3. Carcione JM, Seriani G (1994) Torsional oscillations of anisotropic hollow circular cylinders. Acoust Lett 18(6):439–446
4. Kudlicka J (2006) Dispersion of torsional waves in thick-walled transversely isotropic circular cylinder of infinite length. J Sound Vib 294:368–373
5. Huiling Z, Xiaochun Y (2007) Guided circumferential waves in double-walled carbon nanotubes. Acta Mech Solida Sin 20(2):110–116
6. Xu L, Fan H, Zhou Y (2017) Torsional wave in a circular microtube with clogging attached to the inner surface. Acta Mech Solida Sin 30(3):299–305
7. Kim JO, Chun HY (2003) Interaction between the torsional vibration of a circular rod and an adjacent viscous fluid. J Vib Acoust 125(1):39–45
8. Kim JO, Chun HY (2010) Effect of a viscous fluid at the end face on the torsional vibration of a rod. J Mech Sci Technol 24(2):505–512
9. Abassi W, El Baroudi A, Razafimahery F (2016) Torsional vibrations of fluid-filled multilayered transversely isotropic finite circular cylinder. Int J Appl Mech 8(3):1–14
10. Mnassri I, El Baroudi A, Razafimahery F (2017) Vibrational frequency analysis of finite elastic tube filled with compressible viscous fluid. Acta Mech Solida Sin 30(4):435–444
11. Kim JO, Bau HH (1989) Instrument for simultaneous measurement of density and viscosity. Rev Sci Instrum 60(6):1111–1115
12. Lakes RS (2004) Viscoelastic measurement techniques. Rev Sci Instrum 75(4):797–810
13. Brust M, Schaefer C, Doerr R, Pan L, Garcia M, Arratia PE, Wagner C (2013) Rheology of human blood plasma: viscoelastic versus Newtonian behavior. Phys Rev Lett 110(7):078305
14. Cegla FB, Cawley P, Lowe MJS (1986) Material property measurement using the quasi-Scholte mode: a waveguide sensor. J Acoust Soc Am 26(5):367–372
15. Harrold RT, Sanjana ZN (2005) Acoustic waveguide monitoring of the cure and structural integrity of composite materials. Polym Eng Sci 117(3):1098–1107
16. Roth W, Rich SR (1953) A new method for continuous viscosity measurement. General theory of the ultra-viscoson. J Appl Phys 24(940):940–950
17. Lynnworth LC (1978) New designs for magnetostrictive probes using extensional, torsional and flexural waves. In: Ultrasonics symposium, pp 300–304
18. Joseph DD (1990) Fluid dynamics of viscoelastic liquids. Springer, Berlin
19. Martin SJ, Ricco AJ, Niemczyk TM, Frye GC (1989) Characterization of SH acoustic plate mode liquid sensors. Sens Actuators 20(3):253–268
20. Pelton M, Chakraborty D, Malachosky E, Guyot-Sionnest P, Sader JE (2013) Viscoelastic flows in simple liquids generated by vibrating nanostructures. Phys Rev Lett 111:244502
21. Galstyan V, Pak OS, Stone HA (2015) A note on the breathing mode of an elastic sphere in Newtonian and complex fluids. Phys Fluids 27:032001
22. Zeng XH, Ericsson T (1996) Anisotropy of elastic properties in various aluminium–lithium sheet alloys. Acta Mater 44(5):1801–1812